J Exp Biol Advance Online Articles. First posted online on 15 June 2016 as doi:10.1242/jeb.139139
Access the most recent version at http://jeb.biologists.org/lookup/doi/10.1242/jeb.139139

Intuitive representation of photopolarimetric data using the polarization ellipse

Yakir Luc Gagnon[1,*], Nicholas Justin Marshall[1]

[1]Queensland Brain Institute, University of Queensland

[*] Corresponding author, 12.yakir@gmail.com

Keywords: Photopolarimetry, Circular polarization, Polarization ellipse, Biology, Biomedicine

© 2016. Published by The Company of Biologists Ltd.

Journal of Experimental Biology • Advance article

2 Summary statement

A concise and intuitive way of representing photopolarimetric data that includes circular polarization as well as linear.

3 Abstract

Photopolarimetry is the spatial characterization of light polarization. Unlike intensity or wavelength, we are largely insensitive to polarization and therefore find it hard to explore the multidimensional data that photopolarimetry produces (two spatial dimensions plus four polarization dimensions). Many different ways for presenting and exploring this modality of light have been suggested. Most of these ignore circular polarization, include multiple image-panes that make correlating structure with polarization difficult, and obscure the main trends with overly detailed information and often misleading colour maps. Here, we suggest a novel way for presenting the main results from photopolarimetric analyses. By superimposing a grid of polarization ellipses onto the RGB image, the full polarization state of each cell is intuitively conveyed to the reader. This method presents linear and circular polarization as well as ellipticity in a graphical manner, does not require multiple panes, facilitates the correlation between structure and polarization, and requires the addition of only three novel colours. We demonstrate its usefulness in a biological context where we believe it would be most relevant.

4 Introduction

Photopolarimetric data – spatially resolved information about the polarization of light – is useful for humans. Polarization allows us to gain knowledge about our environment that is inaccessible using light intensity and wavelength alone. Photopolarimetric data is used in ellipsometry (Azzam and Bashara, 1987), remote sensing (Tyo et al., 2006; Halajian and Hallock, 1972; Walraven, 1977; Egan et al., 1991), structure analysis (Zappa et al., 2008), microscopy (Mickols et al., 1985), machine vision (Wolff and Boult, 1991; Wolff et al., 1997), target detection in scattering media (Tyo et al., 1996; Rowe et al., 1995), astronomy (Hough, 2006), and biology as well as biomedical sciences (York et al., 2014). Many invertebrate (Nilsson et al., 1987; Nilsson and Warrant, 1999; Marshall et al., 1991; Horváth, 2014) and some

Journal of Experimental Biology • Advance article

vertebrate species (Phillips and Waldvogel, 1988; Hawryshyn, 1992) have also invested in polarization vision and use it for navigation (Rossel, 1989; Wehner, 2001; Hawryshyn, 1992; Flamarique and Hawryshyn, 1997; Schwind, 1991; Krapp, 2014; Heinze, 2014; el Jundi et al., 2014), predation (Lythgoe, 1967; Shashar et al., 1995, 1998, 2000, 2002), and communication (Horváth, 2014; Cronin et al., 2003; Shashar and Cronin, 1996; Shashar and Hanlon, 1997; Shashar et al., 2002; Mäthger and Denton, 2001; Sweeney et al., 2003). Specifically imaging circular polarization has been found by some biomedical studies as to be useful in diagnosing cancer (Antonelli et al., 2010). Recent findings suggest that humans are capable of some form of polarization sensitivity as well (Temple et al., 2015). Human sensitivity does not however extend to functionally discriminating and spatially resolving the polarization of light. We therefore have to resort to displaying the polarization of light in some other modality that we *do* perceive.

Displaying imagery of partial polarization is problematic because (other than the two spatial dimensions, $x \times y$) at least four variables are needed to fully characterize it. While many different interpretations for polarization exist, one of the most common used is (see Table 1 for a list of abbreviations): intensity ($0 < I < \infty$), degree of linear polarization ($0 \leq DoLP \leq 1$), angle of linear polarization ($-90° \leq AoLP < 90°$), and degree of circular polarization ($-1 \leq DoCP \leq 1$).

Presenting photopolarimetric data has had different approaches (Yemelyanov et al., 2003b; Tyo et al., 1998; Wolff et al., 1997; Bernard and Wehner, 1977; Solomon, 1981; Engheta and Pugh Jr, 2002; Yemelyanov et al., 2003a). While some of these suggestions include unique ways to present the extra dimensions needed (e.g. movement (Yemelyanov et al., 2003b)), most photopolarimetric data is presented as a set of 3–5 image-panes each describing one of the polarization variables using a colour space or gamut available on computers (Figure 5.2). This method suffers from a number of disadvantages:

1. Circular polarization (or ellipticity) is often ignored.

2. When circular polarization is not ignored, it is hard to discern any information about ellipticity and total polarization.

3. Multiple panes are required to display the polarization state in full making it difficult to correlate structures and locations between the different panes.

Journal of Experimental Biology • Advance article

Table 1: A table of abbreviations used in this study.

Abbreviation	Meaning
I	Intensity
DoLP	Degree of Linear Polarization
AoLP	Angle of Linear Polarization
DoCP	Degree of Circular Polarization
$s_{0...3}$	Stokes parameters
s_0^{UP}	Unpolarized component of light
s_0^{P}	Polarized component of light
a	Minor axis of the polarization ellipse
b	Major axis of the polarization ellipse
R	Ratio between the minor and major axes
θ	Angle of Linear Polarization
h	Handedness of the polarization ellipse
P	Ratio between the total and polarized light
RGB	Red, Green, and Blue

4. Richly coloured panes obscure rather than convey the main trends in the data.

5. Edge artefacts are common and conspicuous, distracting the reader from the main point.

6. Small angular differences in AoLP are difficult to discern.

These shortcomings are especially evident when presenting biological photopolarimetric data. Biologists are often interested in patches and areas with similar polarization (rather than small scale variations), they require information about circular and elliptical polarization, and they want to correlate the polarization with the body segments or markings on the organism. Here we suggest a new polarimetry representation that both improves on the shortcomings of the traditional method and answers most of the needs biologists and biomedical imaging may have.

Journal of Experimental Biology • Advance article

5 Materials and methods

5.1 Polarization ellipse

In this study, polarization is represented using the polarization ellipse (Collett, 1992). While the polarization ellipse is mostly used as a graphical representation of purely polarized light (either monochromatic incoherent radiation or a single electromagnetic wave), it can be adapted to describe partly polarized light by scaling the ellipse in proportion to the total polarization of the light.

The shape of the polarization ellipse (its minor and major axes and its orientation angle) are dictated by the Stokes parameters. These four parameters are often combined into a vector, the Stokes vector, which fully describes the polarization state of electromagnetic radiation in a mathematically convenient way. Stokes parameters are also easy to experimentally measure, each resulting from the addition or subtraction of a few light measurements. For instance, the first Stokes parameter simply describes the total intensity of the light (the reader is directed to any optics literature for further details about Stokes mathematics).

Because of the additive property of Stokes vectors a partially polarized beam of light can be decomposed into its unpolarized and (completely) polarized components :

$$\begin{bmatrix} s_0 \\ s_1 \\ s_2 \\ s_3 \end{bmatrix} = \begin{bmatrix} s_0^{\mathrm{UP}} \\ 0 \\ 0 \\ 0 \end{bmatrix} + \begin{bmatrix} s_0^{\mathrm{P}} \\ s_1 \\ s_2 \\ s_3 \end{bmatrix}, \; s_0^{\mathrm{P}} = \sqrt{s_1^2 + s_2^2 + s_3^2} \tag{1}$$

where s_0^{UP} is the unpolarized portion of the light and s_0^{P} is the polarized part. We will calculate the shape of the polarization ellipse using these two Stokes vectors. The shape of the ellipse depends on the ratio between the minor and major axes of the ellipse, R, the orientation angle (i.e. angle of polarization) of the ellipse, θ, and its handedness, h. Following are the mathematical relationships between these variables and the Stokes parameters of a partially

polarized beam of light (Collett, 1992):

$$R = \frac{s_0^{\mathrm{P}} - \sqrt{s_1^2 + s_2^2}}{s_0^{\mathrm{P}} + \sqrt{s_1^2 + s_2^2}} \tag{2}$$

$$\theta = \frac{1}{2} \arctan \frac{s_2}{s_1} \tag{3}$$

$$h = \mathrm{sign}\,(s_3) \tag{4}$$

Since the degree of polarization will be depicted by the size of the ellipse, we need to scale the ellipse's axes. Therefore, the minor, a, and major b, axes are scaled by the ratio, P, of the polarized light intensity, s_0^{P}, to the total light intensity, s_0:

$$P = \frac{s_0^{\mathrm{P}}}{s_0} \tag{5}$$

$$a = P \cdot R \tag{6}$$

$$b = P \tag{7}$$

Note that since both axes are scaled by the polarization ratio P, the actual intensity of the light (i.e. s_0) has no bearing on the shape of the ellipse.

5.2 Photopolarimetry

The suggested presentation of polarimetric data in this study follows these general steps:

Journal of Experimental Biology • Advance article

1. Spatially resolved polarimetric data is collected photographically.
2. This data is divided into a grid of cells.
3. At each cell:
   (a) The mean Stokes vector is used to calculate the parameters of a polarization ellipse.
   (b) This ellipse is superimposed on an image of the subject matter at the cell centre.

While a methodological description of how photopolarimetric data should be collected (i.e. photopolarimetry) is outside the scope of this study, we describe briefly how we collected our photopolarimetric data (see more information in Horváth, 2014; Wolff, 1997). A Nikon D300 (with a Nikon 105 mm micro lens) was fitted with two rotatable filter rings. One ring had a linear polarizing film while the other had a quarter-wave retarder film (both from American Polarizers, Reading, USA). By rotating these two rings (relative to each other and the camera's objective) the six required measurements for calculating the polarization state were obtained (horizontal, vertical, diagonal, anti-diagonal, right hand circular, and left hand circular). Rotating the filters and taking the six pictures took about 30–60 seconds. This relatively manual procedure can be made quicker with the use of motorized filters, splitting the image into separate sensors, or etching orthogonal filters onto a thin film that is then aligned to the sensor's pixels (Gruev et al., 2010). In order to maintain the linear relationship between light intensity and pixel intensity, the images were saved in raw format. Converting the raw NEF files was done with `dcraw` (an open-source program which reads raw image formats and converts these into the standard PPM and TIFF image formats). All image processing was done in `Julia` (Bezanson et al., 2014) (an open-source, high-level, high-performance dynamic programming language for technical computing). Superimposing the ellipses on the RGB image was done with LaTeX(and the Ti*k*Z package). All the code used in this procedure is freely available on `github` (`https://github.com/yakir12/polarimetryLab`).

The grid's cell size was chosen so that the resulting cells are not too small to be discernible while at the same time are not too big as to include too many imaged structures. Total polarization is encoded by the size of the ellipse (as previously discussed), and handedness is illustrated by the ellipse's colour (two different colours). When the eccentricity of the ellipse

Journal of Experimental Biology • Advance article

is below a certain threshold and its shape is practically a line, handedness is less relevant and the ellipse is coloured with a third colour.

To better asses the functionality of our method, we constructed a custom polarization standard. This standard contained six squares (see Figures 2): black and white polyester felt at the top, vertically and horizontally oriented polaroids in the middle, and left hand and right hand circularly polarized filters at the bottom (all filters are from American Polarizers, Reading, USA). Finally, all the animal photography in this report was done under the approval and oversight of the UQ Native and Exotic Wildlife and Marine Animals (NEWMA) Animal Ethics Committee.

Journal of Experimental Biology • Advance article

6 Results and discussion

The proposed method tackled all of the shortcomings described in the Introduction (disadvantages 1–6). Since information about circular polarization is intrinsic to the polarization ellipse it is never ignored in our method.

The polarization ellipse intuitively presents information about the ellipticity of the light, allowing the viewer to get an overview of this modality of light. We can see for example that the two bottom circularly polarized filters in the standard in Figure 2 slightly differ in ellipticity (i.e. the left hand circular polarized filter is less elliptical than the right hand circular polarized filter). This difference is however not as evident in the traditional presentation of photopolarimetric data in Figure 5.2 and would require a comparison of intensities between the DoLP and DoCP panes (note that the DoLP of the right hand circular polarized filter is indeed higher than that of the left hand circular polarized filter).

With our method, there is no need for multiple panes to display the polarization state which facilitates the interpretation of the data. It is easy to correlate polarization with body segment or marking on the subject organism (e.g. the red tail, legs, and head of the mantis shrimp in Figure 3).

Only three novel colours are needed to convey information about the polarization in full. Less novel colours are needed in cases where the scene contains only linear, left hand circular, or right hand circular polarization.

Edge artefacts are removed due to the averaging that occurs within each grid cell, facilitating natural images where objects constantly move (the fern in Figure S2) or the stability of the photopolarimetry is compromised. Apart

Journal of Experimental Biology • Advance article

from reducing edge artifacts, averaging results in smaller and less conspicuous ellipses in grid-cells that contain asimilar Stokes vectors (i.e. the differences in the Stokes parameters between the pixels are large). This effect is caused by the fact that the mean degree of polarization of a set of heterogeneous Stokes vectors approaches zero. Therefore, averaging actually highlights patches that have similar polarization properties, facilitating the detection of biologically relevant patches. This is noticeable, for example, in the lack of any ellipses in the dark and noisy background of the beetle in Figure S3.

Angular data is presented contextually with directional shapes making any interpretation intuitive and easy. For example, note how easily one can discern the vertical and horizontal AoLP in the two middle polaroid filters in Figure 2 while the equivalent interpretation in the conventional presentation of photopolarimetric data in Figure 5.2 requires checking the legend. Additionally, the directionality of the polarization ellipse brings to light novel angular patterns: note the concentric directional pattern of the elliptically polarized light reflecting from the beetle's sides in Figure S3. Finally, directionality is only discernible when it is most relevant, i.e. when linear polarization is stronger than circular polarization. Notice how the radiating pattern of ellipses is visible at the periphery of the beetle's body in Figure S3 while any such pattern is not as discernible in the centre of the beetle's body where the polarization is mostly circular.

By removing the colour scales traditionally needed for DoLP, AoLP, and DoCP we reduce interpretation error associated with trying to scale variables over false-colour gamuts (Rogowitz and Treinish, 1998). One can see a clear example of all of these advantages when comparing our suggested presentation of photopolarimetric data in Figure 3 to the conventional presentation in Figure S1. It is difficult to get a sense of the location (on the body of the animal), degree, and orientation (AoLP) of the ellipticity in the traditional presentation of photopolarimetric data. Edge artefacts are numerous and make the interpretation of the DoLP pane cumbersome. The current method for displaying photopolarimetric data (Figure 3) overcomes most of these difficulties.

While this method is useful it does suffer from a number of limitations. Polarization details that are smaller than the grid cell are not visible due to the averaging within the cell. Smaller cells may help in this respect, but reducing the cell size beyond a certain point may prevent the reader from seeing the polarization ellipses. A simple solution may be to include a zoomed-in

Journal of Experimental Biology • Advance article

section of the area of interest. As mentioned before, there is an intrinsic relationship between circular polarization and angular variation: when DoCP is much higher than DoLP the polarization ellipse becomes a circle. Due to this relationship, it may become difficult to gather information about the AoLP in such cases. It is however important to consider that for relatively high DoCP AoLP may not be so relevant. A similar relationship exists with degree of total polarization: the lower the degree of total polarization the smaller the polarization ellipse is going to be and the harder it is to see the shape of the ellipse. The same logic can be applied here as well, polarization characteristics are less important at very low polarizations. Finally, it is important to note that this method does not attempt (and consequently fails) to simultaneously give the reader access to the raw data *and* present the main trends in the data. Instead, this method concentrates on the latter task – efficiently presenting the reader with the main photopolarimetric trends.

Apart from adjusting the grid cell size, this method can be modified in other ways to better suit each case-study. The colors encoding handedness and linearity can be adjusted to increase/decrease contrast depending on the existing colors in the background image (note the usage of different colours in Figures 2 – 3). One could couple the opacity of the polarization ellipse to the degree of total polarization to make it even clearer which part of the image is more polarized. Eccentricity can also be made to inversely control the saturation of the polarization ellipse's colors. This makes sense because handedness information is less relevant at high eccentricities. Instead of the current linear relationship between the ellipse parameters and the polarization state (e.g. ellipse size and degree of total polarization), one could employ a nonlinear relationship. While the exact mechanism of polarization vision is not fully understood, a logarithmic relationship between the degree of polarization and the size of the polarization ellipse may better emulate a biological visual system (How and Marshall, 2014). One can divide the parameters of the polarization ellipse into a small number of discrete categories to facilitate and accelerate the comparison between available polarization states in the image. Finally, since the polarization data is not conveyed by the colors or intensities of the background image the colors and intensities of the image of the subject-matter may be adjusted to maximally suit the presentation of the data. These adjustments may include enhanced color saturation (the red colouring of the mantis shrimp in Figure 3 were saturated to enhance the apparent correlation between red pigmentation and circular polarization), white

balance, different brightness responses or ranges, colorblind suited, anaglyph 3D effects, etc.

We suggested an efficient way of displaying the main trends in photopolarimetric data by superimposing a grid of polarization ellipses on the image. This method improves on the more traditional way of displaying photopolarimetric data. Most of these improvements will attract scientists in biology and biomedicine but may also be relevant in other disciplines.

7 Acknowledgements

The authors would like to thank the Air Force Office of Scientific Research, the Asian Office of Aerospace Research and Development, and the Australian Research Council for financial support. We would also like to thank Dr. David Merritt, Chris Moeseneder, and Justin S. Bartlett for access, identification, and helpful insight with the beetles used in this study.

8 Competing interests

The authors do not have any competing interests.

9 Author contributions

Conceptualization Ideas, Y.L.G. and N.J.M.; Methodology, Y.L.G.; Software, Y.L.G.; Formal Analysis, Y.L.G.; Resources, Y.L.G. and N.J.M.; Writing Original Draft, Y.L.G.; Writing Review & Editing, Y.L.G. and N.J.M.; Visualization, Y.L.G.; Supervision, N.J.M.; Funding Acquisition, N.J.M.

10 Funding

Australian Research Council (FL140100197); Air Force Office of Scientific Research (FA2386-13-1-4134)

Journal of Experimental Biology • Advance article

References

Antonelli, M.-R., Pierangelo, A., Novikova, T., Validire, P., Benali, A., Gayet, B. and De Martino, A. (2010). Mueller matrix imaging of human colon tissue for cancer diagnostics: how monte carlo modeling can help in the interpretation of experimental data. *Optics express* **18**, 10200–10208.

Azzam, R. M. and Bashara, N. M. (1987). *Ellipsometry and polarized light*. North-Holland. sole distributors for the USA and Canada, Elsevier Science Publishing Co., Inc.

Bernard, G. D. and Wehner, R. (1977). Functional similarities between polarization vision and color vision. *Vision research* **17**, 1019–1028.

Bezanson, J., Edelman, A., Karpinski, S. and Shah, V. B. (2014). Julia: A fresh approach to numerical computing. *CoRR* **abs/1411.1607**, 1–37.

Collett, E. (1992). *Polarized light. Fundamentals and applications*. Optical Engineering, New York: Dekker,— c1992.

Cronin, T. W., Shashar, N., Caldwell, R. L., Marshall, J., Cheroske, A. G. and Chiou, T.-H. (2003). Polarization vision and its role in biological signaling. *Integrative and Comparative Biology* **43**, 549–558.

Egan, W. G., Johnson, W. and Whitehead, V. (1991). Terrestrial polarization imagery obtained from the space shuttle: characterization and interpretation. *Applied optics* **30**, 435–442.

el Jundi, B., Smolka, J., Baird, E., Byrne, M. J. and Dacke, M. (2014). Diurnal dung beetles use the intensity gradient and the polarization pattern of the sky for orientation. *Journal of Experimental Biology* **217**, 2422–2429.

Engheta, N. and Pugh Jr, E. N. (2002). Biologically motivated representational schemes for mapping polarization information into visual information. Technical report, DTIC Document.

Journal of Experimental Biology • Advance article

Flamarique, I. N. and Hawryshyn, C. W. (1997). Is the use of underwater polarized light by fish restricted to crepuscular time periods? *Vision research* **37**, 975–989.

Gruev, V., Perkins, R. and York, T. (2010). Ccd polarization imaging sensor with aluminum nanowire optical filters. *Optics express* **18**, 19087–19094.

Halajian, J. and Hallock, H. (1972). Principles and techniques of polarimetric mapping. In *Remote Sensing of Environment, VIII*, volume 1, p. 523.

Hawryshyn, C. W. (1992). Polarization vision in fish. *American Scientist* **80**, 164–175.

Heinze, S. (2014). Polarized-light processing in insect brains: Recent insights from the desert locust, the monarch butterfly, the cricket, and the fruit fly. In *Polarized Light and Polarization Vision in Animal Sciences*, pp. 61–111. Springer.

Horváth, G. (2014). *Polarized light and polarization vision in animal sciences*. Springer.

Hough, J. (2006). Polarimetry: a powerful diagnostic tool in astronomy. *Astronomy & Geophysics* **47**, 3–31.

How, M. J. and Marshall, N. J. (2014). Polarization distance: a framework for modelling object detection by polarization vision systems. *Proceedings of the Royal Society of London B: Biological Sciences* **281**, 20131632.

Krapp, H. G. (2014). Sensory integration: neuronal filters for polarized light patterns. *Current Biology* **24**, R840–R841.

Lythgoe, J. (1967). Polarized light and underwater vision. *Nature* **213**, 893–894.

Marshall, N., Land, M., King, C. and Cronin, T. (1991). The compound eyes of mantis shrimps (crustacea, hoplocarida, stomatopoda). I. compound eye structure: the detection of polarized light. *Philosophical Transactions of the Royal Society B: Biological Sciences* **334**, 33–56.

Journal of Experimental Biology • Advance article

Mäthger, L. and Denton, E. (2001). Reflective properties of iridophores and fluorescent 'eyespots' in the loliginid squid *Alloteuthis subulata* and *Loligo vulgaris*. *Journal of Experimental Biology* **204**, 2103–2118.

Mickols, W., Tinoco, I., Katz, J. E., Maestre, M. F. and Bustamante, C. (1985). Imaging differential polarization microscope with electronic readout. *Review of scientific instruments* **56**, 2228–2236.

Nilsson, D.-E., Labhart, T. and Meyer, E. (1987). Photoreceptor design and optical properties affecting polarization sensitivity in ants and crickets. *Journal of Comparative Physiology A* **161**, 645–658.

Nilsson, D.-E. and Warrant, E. J. (1999). Visual discrimination: Seeing the third quality of light. *Current biology* **9**, R535–R537.

Phillips, J. B. and Waldvogel, J. A. (1988). Celestial polarized light patterns as a calibration reference for sun compass of homing pigeons. *Journal of Theoretical Biology* **131**, 55–67.

Rogowitz, B. E. and Treinish, L. A. (1998). Data visualization: the end of the rainbow. *Spectrum, IEEE* **35**, 52–59.

Rossel, S. (1989). Polarization sensitivity in compound eyes. In *Facets of vision*, pp. 298–316. Springer.

Rowe, M., Tyo, J., Engheta, N. and Pugh, E. (1995). Polarization-difference imaging: a biologically inspired technique for observation through scattering media. *Optics Letters* **20**, 608–610.

Schwind, R. (1991). Polarization vision in water insects and insects living on a moist substrate. *Journal of Comparative Physiology A* **169**, 531–540.

Shashar, N., Adessi, L. and Cronin, T. (1995). Polarization vision as a mechanism for detection of transparent objects. *Ultraviolet radiation and coral reefs, HIMB Tech. Rept* **41**, 207–211.

Shashar, N. and Cronin, T. W. (1996). Polarization contrast vision in octopus. *The Journal of Experimental Biology* **199**, 999–1004.

Shashar, N., Hagan, R., Boal, J. G. and Hanlon, R. T. (2000). Cuttlefish use polarization sensitivity in predation on silvery fish. *Vision research* **40**, 71–75.

Journal of Experimental Biology • Advance article

Shashar, N., Hanlon, R. and Petz, A. (1998). Polarization vision helps detect transparent prey. *Nature* **393**, 222–223.

Shashar, N. and Hanlon, R. T. (1997). Squids (*Loligo pealei* and *Euprymna scolopes*) can exhibit polarized light patterns produced by their skin. *The Biological Bulletin* **193**, 207.

Shashar, N., Milbury, C. and Hanlon, R. (2002). Polarization vision in cephalopods: neuroanatomical and behavioral features that illustrate aspects of form and function. *Marine and Freshwater Behaviour and Physiology* **35**, 57–68.

Solomon, J. E. (1981). Polarization imaging. *Applied Optics* **20**, 1537–1544.

Sweeney, A., Jiggins, C. and Johnsen, S. (2003). Insect communication: polarized light as a butterfly mating signal. *Nature* **423**, 31–32.

Temple, S. E., McGregor, J. E., Miles, C., Graham, L., Miller, J., Buck, J., Scott-Samuel, N. E. and Roberts, N. W. (2015). Perceiving polarization with the naked eye: characterization of human polarization sensitivity. In *Proc. R. Soc. B*, volume 282, p. 20150338. The Royal Society.

Tyo, J., Pugh, E. and Engheta, N. (1998). Colorimetric representations for use with polarization-difference imaging of objects in scattering media. *JOSA A* **15**, 367–374.

Tyo, J., Rowe, M., Pugh, E. and Engheta, N. (1996). Target detection in optically scattering media by polarization-difference imaging. *Applied Optics* **35**, 1855–1870.

Tyo, J. S., Goldstein, D. L., Chenault, D. B. and Shaw, J. A. (2006). Review of passive imaging polarimetry for remote sensing applications. *Appl. Opt.* **45**, 5453–5469.

Walraven, R. (1977). Polarization imagery. In *21st Annual Technical Symposium*, pp. 164–167. International Society for Optics and Photonics.

Wehner, R. (2001). Polarization vision–a uniform sensory capacity? *Journal of Experimental Biology* **204**, 2589–2596.

Journal of Experimental Biology • Advance article

Wolff, L. B. (1997). Polarization vision: a new sensory approach to image understanding. *Image and Vision computing* **15**, 81–93.

Wolff, L. B. and Boult, T. E. (1991). Constraining object features using a polarization reflectance model. *IEEE Transactions on Pattern Analysis & Machine Intelligence* **7**, 635–657.

Wolff, L. B., Mancini, T., Pouliquen, P., Andreou, A. G. et al. (1997). Liquid crystal polarization camera. *Robotics and Automation, IEEE Transactions on* **13**, 195–203.

Yemelyanov, K. M., Lin, S.-S., Luis, W. Q., Pugh Jr, E. N. and Engheta, N. (2003a). Bio-inspired display of polarization information using selected visual cues. In *Optical Science and Technology, SPIE's 48th Annual Meeting*, pp. 71–84. International Society for Optics and Photonics.

Yemelyanov, K. M., Lo, M., Pugh Jr, E. N., Engheta, N. et al. (2003b). Display of polarization information by coherently moving dots. *Optics express* **11**, 1577–1584.

York, T., Powell, S. B., Gao, S., Kahan, L., Charanya, T., Saha, D., Roberts, N. W., Cronin, T. W., Marshall, J., Achilefu, S. et al. (2014). Bioinspired polarization imaging sensors: from circuits and optics to signal processing algorithms and biomedical applications. *Proceedings of the IEEE* **102**, 1450–1469.

Zappa, C. J., Banner, M. L., Schultz, H., Corrada-Emmanuel, A., Wolff, L. B. and Yalcin, J. (2008). Retrieval of short ocean wave slope using polarimetric imaging. *Measurement Science and Technology* **19**, 055503.

Journal of Experimental Biology • Advance article

Figures

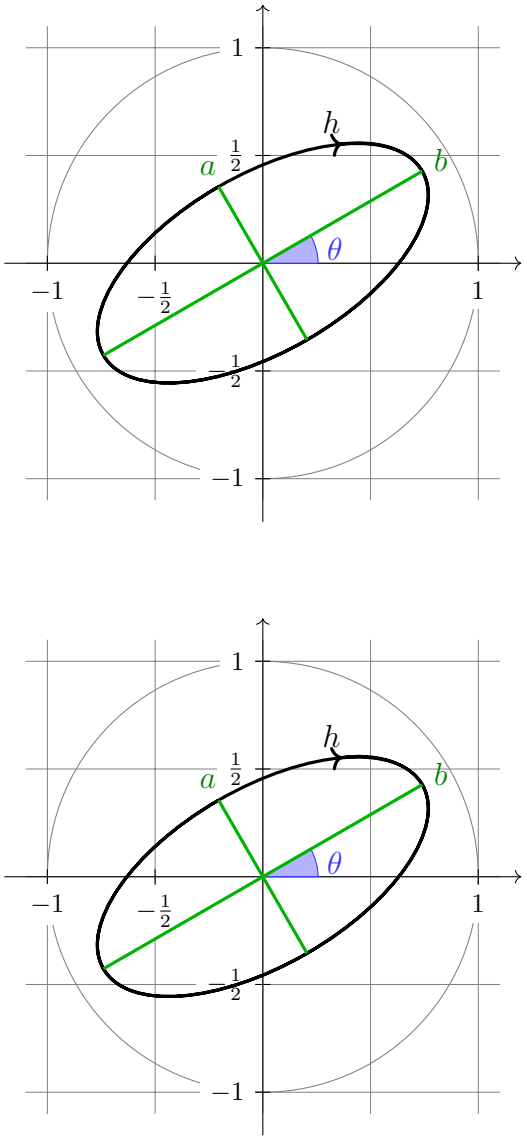

Figure 1: **The polarization ellipse of partly polarized light:** Here, the Stokes parameters $[s_1, s_2, s_3]$ are equal to $[0.15, 0.26, 0.8]$ (arbitrary chosen values) respectively. Using Equations 3–7, we can calculate that the total polarization is 85%, the angle of polarization is 30°, and the two axes are 0.41 and 0.85. The handedness of the light is indicated by the clockwise turning arrow (the light is right-hand circularly polarized). Notice that since the sum of squares of these stoke parameters must be smaller (or equal) to the square of the first Stokes parameter, the ellipse can never be larger than the grey circle (with a radius equal to one).

Journal of Experimental Biology • Advance article

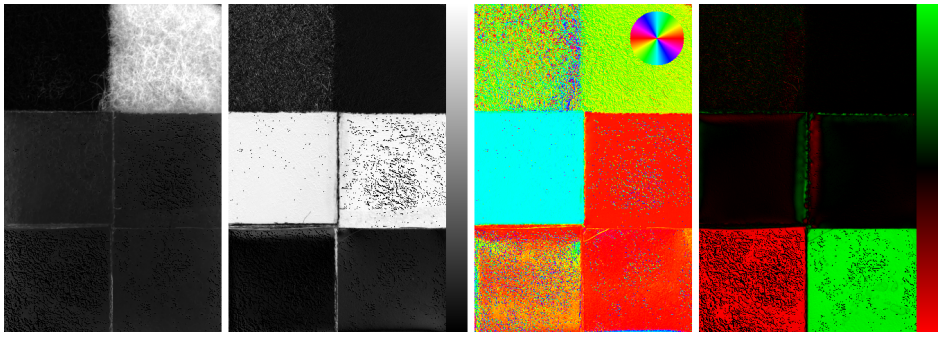

I DoLP AoLP DoCP

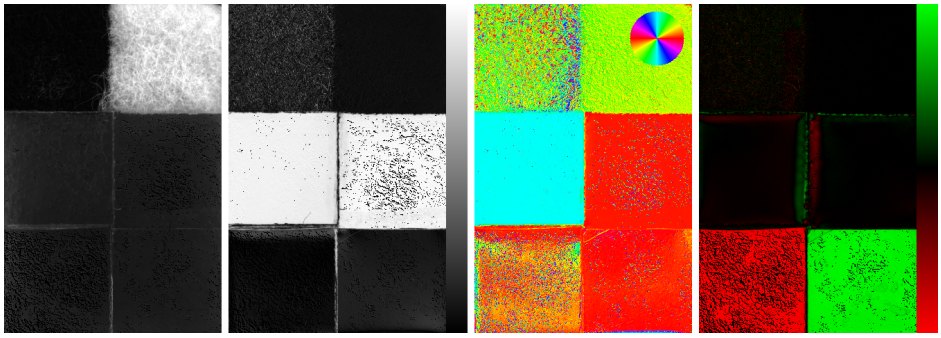

I DoLP AoLP DoCP

Journal of Experimental Biology • Advance article

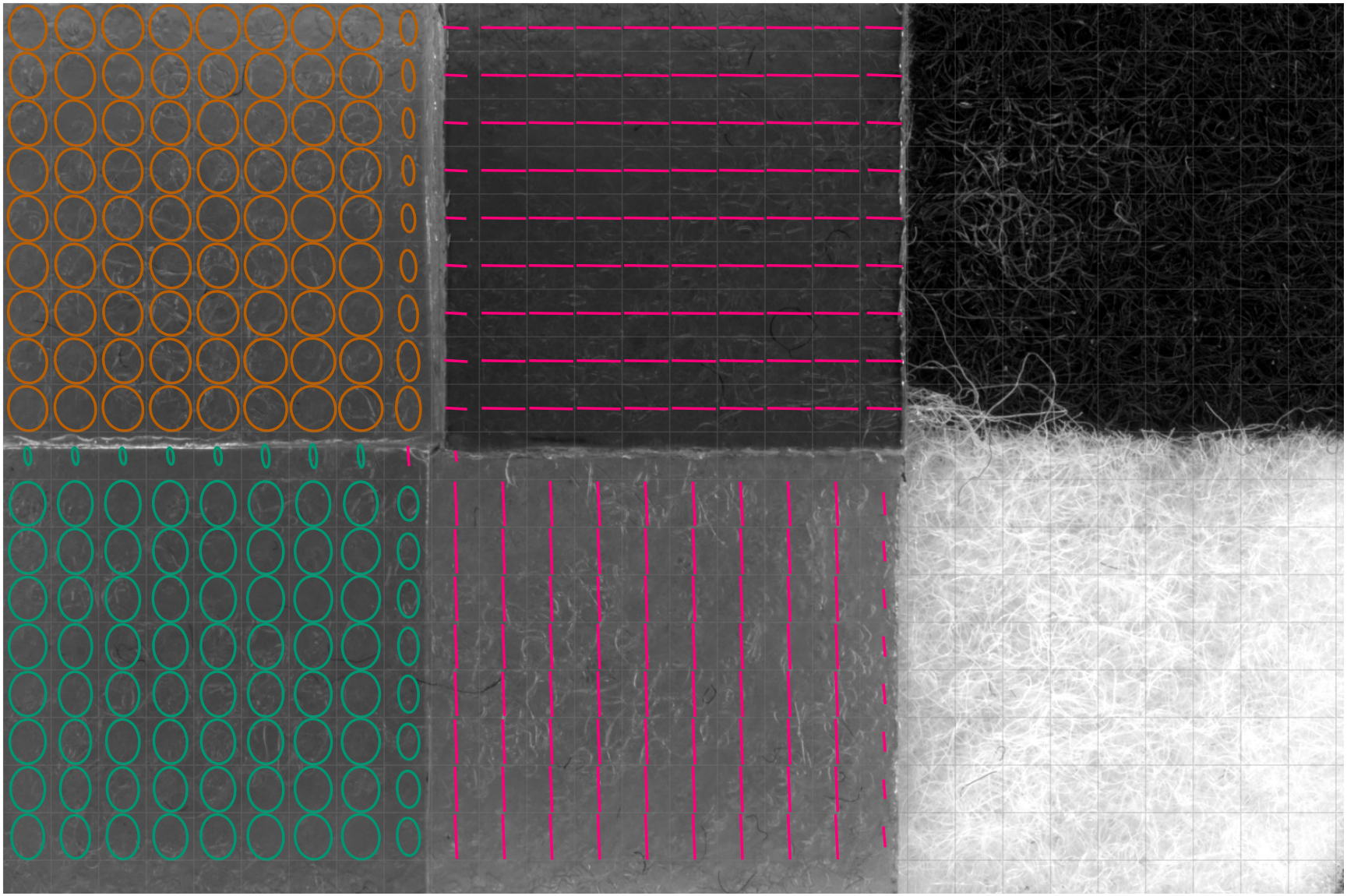

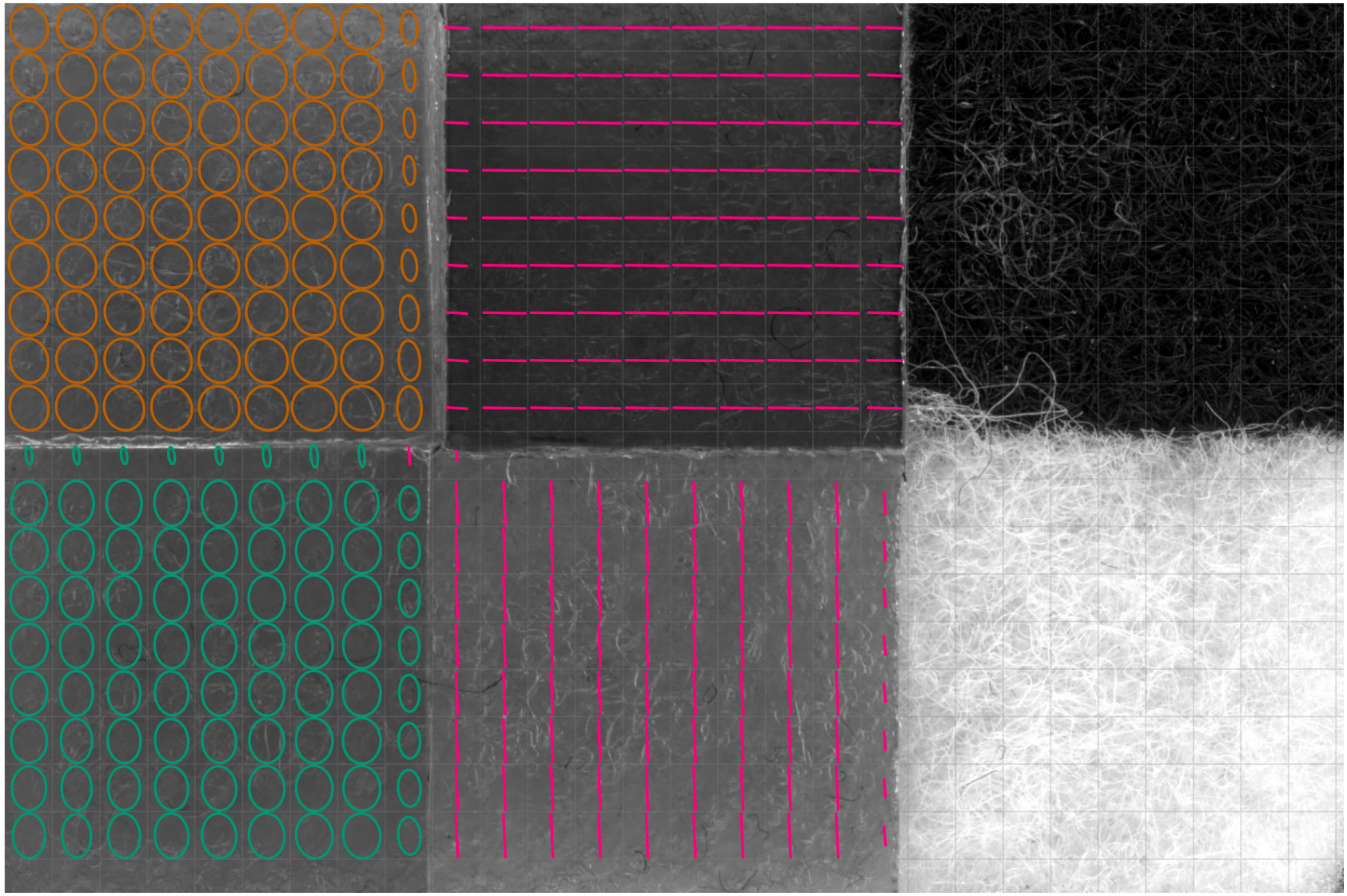

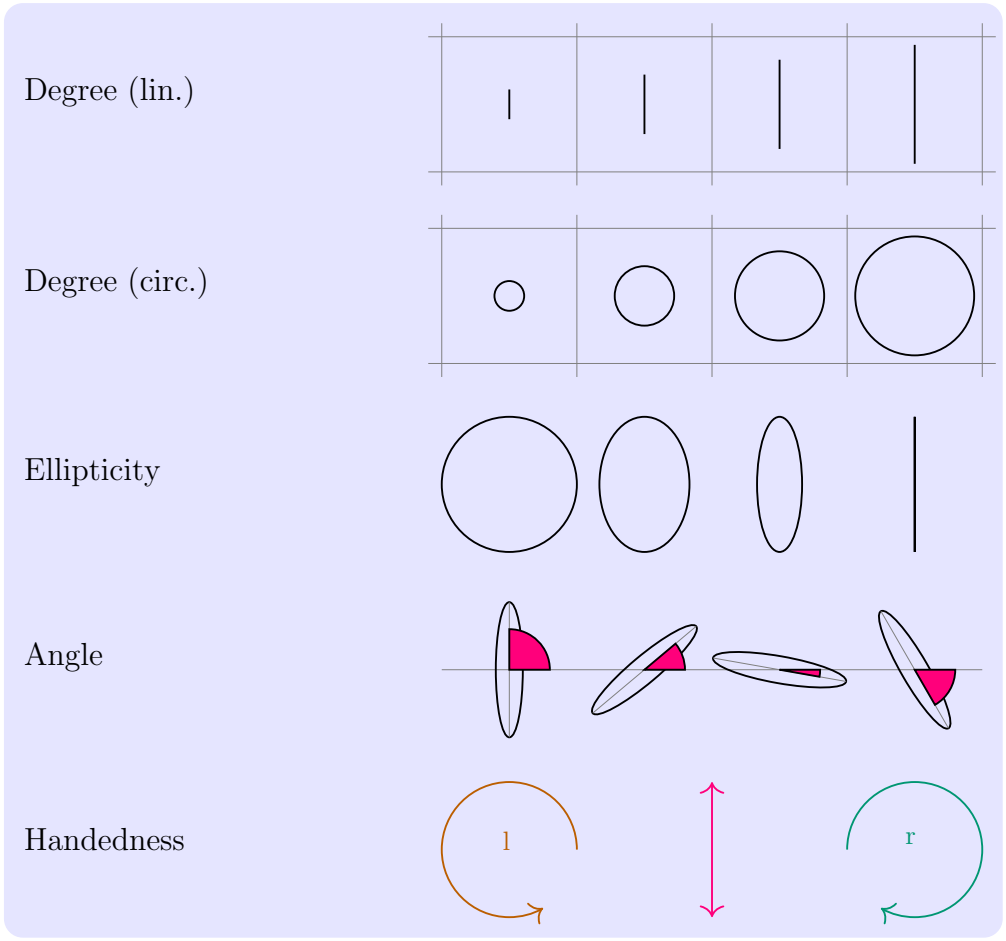

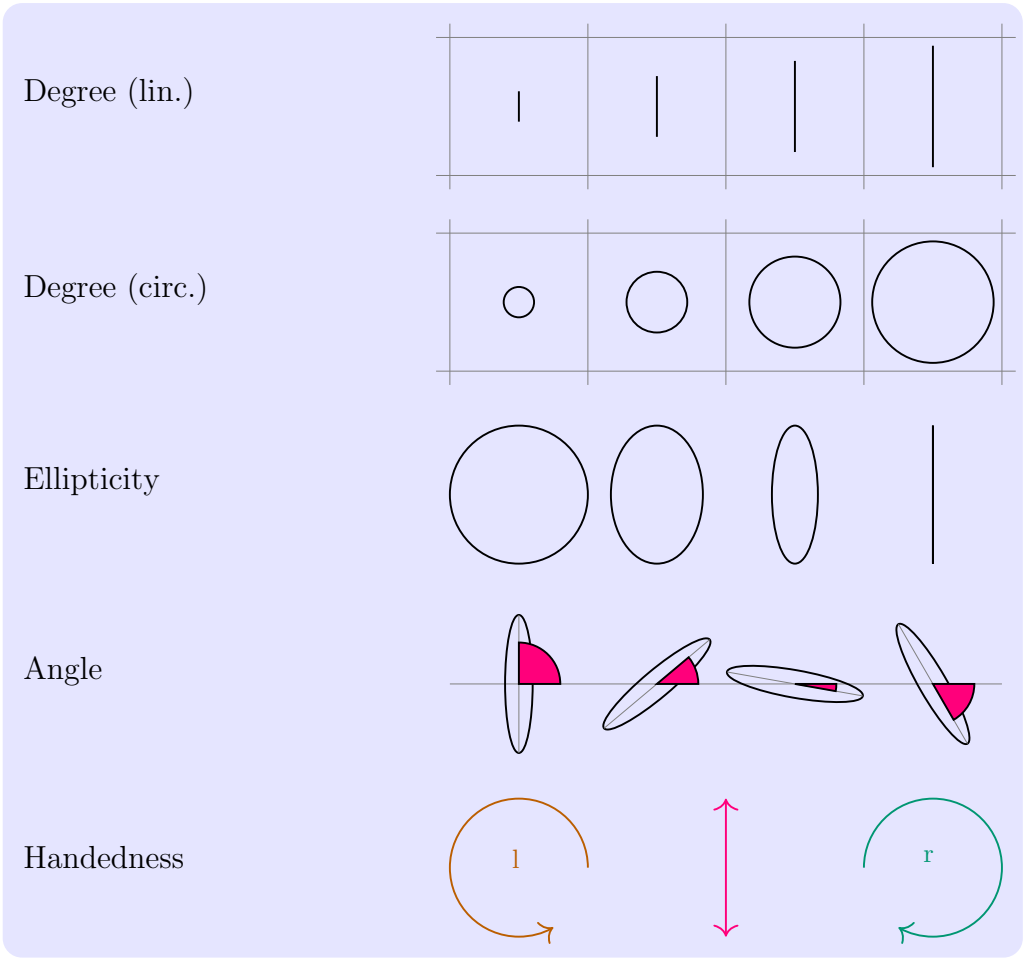

Journal of Experimental Biology • Advance article

Figure 2: **A comparison between the conventional and current presentation of photopolarimetric data of a custom-made polarization standard:** (a) Conventional mulit-pane presentation of photopolarimetric data. The left pane (I) shows the relative (linear) intensity of the light. To the right is the degree of linear polarization (DoLP) and a colour scale where black is linearly unpolarized light and white is 100% linearly polarized light. Next is the angle of linear polarization (AoLP) (notice the circular colour scale at the top right corner). Last to the right is the degree of circular polarization (DoCP) with a colour scale where red is 100% left hand circularly polarized light, black is circularly unpolarized light, and green is 100% right hand circularly polarized light. (b) The current study's method applied to the same standard. The RGB image of the standard was superimposed by a grey grid and polarization ellipses. Polarization that is primarily linear is colour coded with magenta (the threshold was arbitrarily set to an eccentricity of 0.2), left hand circular polarization is colour coded with orange, and right hand circularly polarized light is colour coded with turquoise. A legend on the right explains the meaning of the shape, orientation, and color of the ellipses.

Journal of Experimental Biology • Advance article

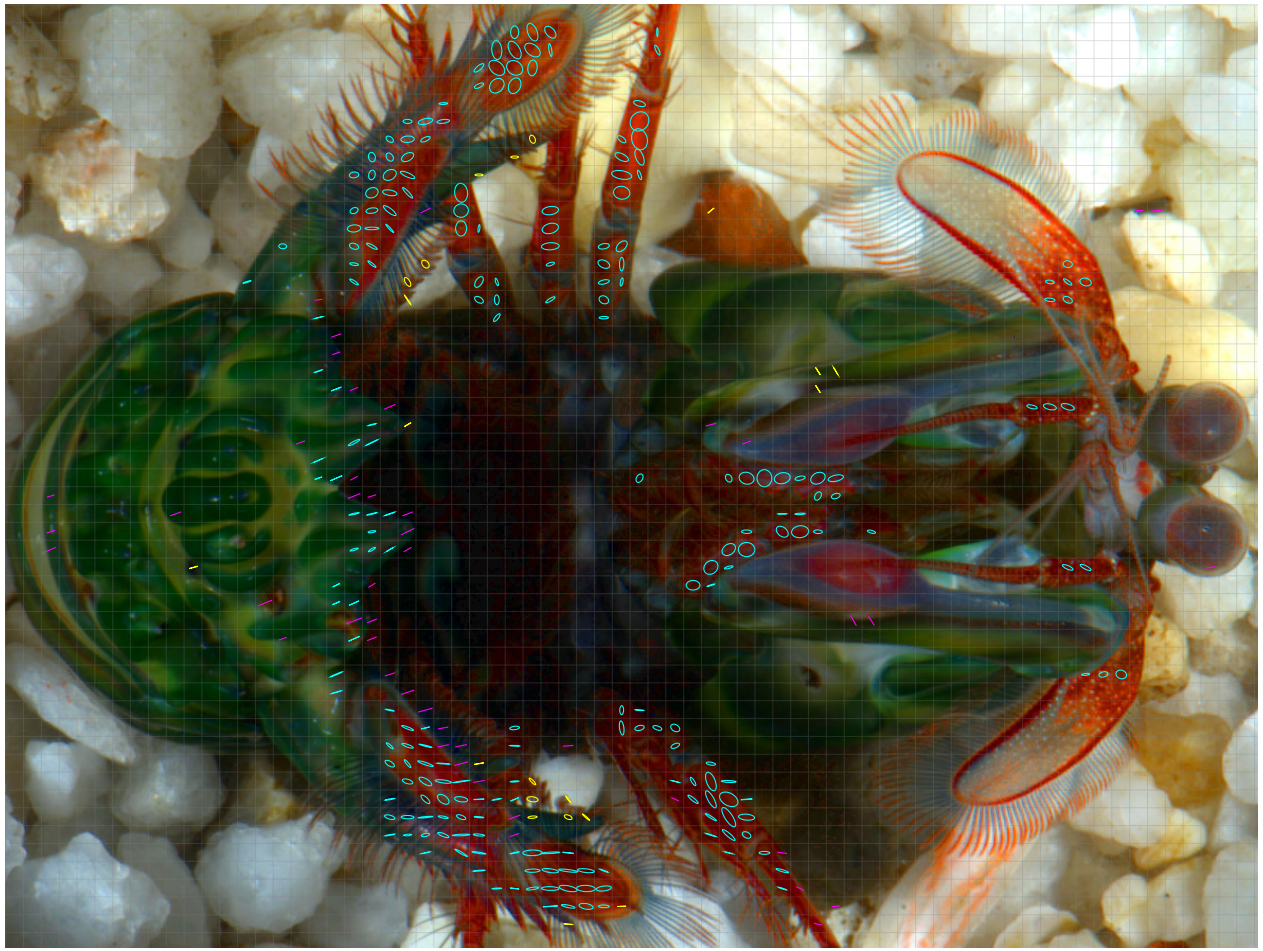

Figure 3: Photopolarimetric data of the stomatopod, *Gonodactylaceus falcatus*, in a defensive position. Since most of the polarization is on the red portions of the head, legs, and tail of the animal, the left hand circularly polarized light is coded with red's complimentary colour, cyan, rare right hand circularly polarized light is coded with yellow, and linearly polarized light is magenta. The red colour in the image was overly saturated to better emphasize the correlation between the red pigmentation and the polarization (compare this figure with the traditional presentation of photopolarimetric data in Figure S1).

Journal of Experimental Biology • Advance article

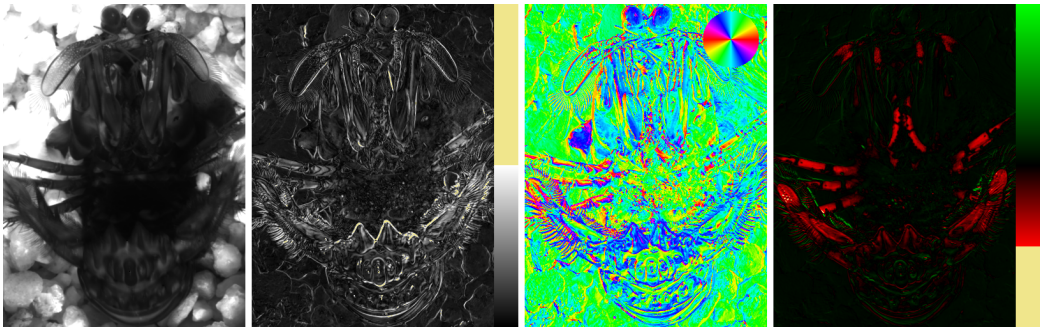

I DoLP AoLP DoCP

Figure S1: Conventional photopolarimetry of the stomatopod, *Gonodactylaceus falcatus*, shown in Figure 3. The left pane (I) shows the relative (linear) intensity of the light. To the right is the degree of linear polarization (DoLP) and a colour scale where black is linearly unpolarized light and white is 50% linearly polarized light. Next is the angle of linear polarization (AoLP) (notice the circular colour scale at the top right corner). Last to the right is the degree of circular polarization (DoCP) with a colour scale where red is 50% left hand circularly polarized light, black is circularly unpolarized light, and green is 100% right hand circularly polarized light. Note how hard it is to appreciate the ellipticity of the polarization and its location on the body of the animal.

Journal of Experimental Biology • Supplementary information

Figure S2: Photopolarimetry of a linearly polarized reflection from the glossy leaves of a fern (*Asplenium nidus*). The linear polarization here is coded with green's complimentary colour, magenta. Although this specimen was photographed during a windy day, the polarization patterns on its leaves are still clear.

Journal of Experimental Biology • Supplementary information

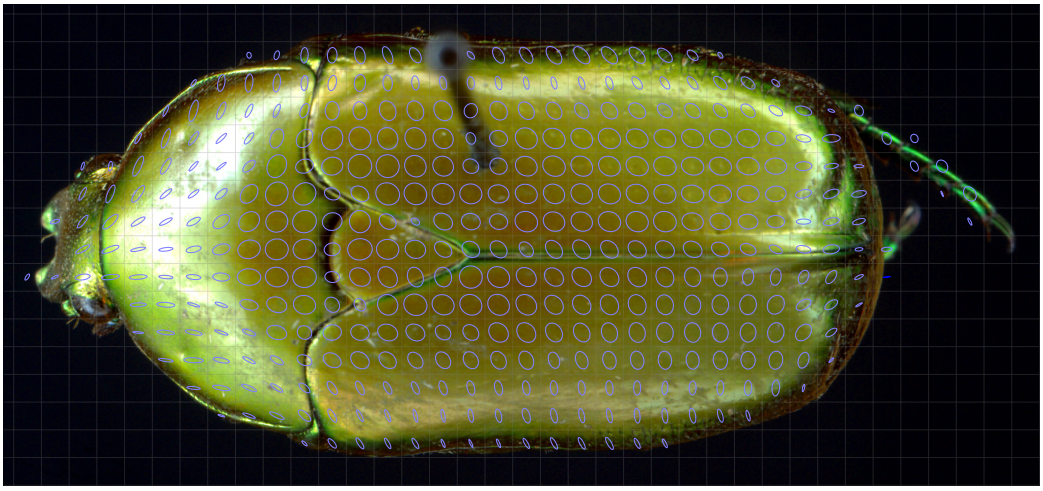

Figure S3: Photopolarimetry of the circularly polarized scarab beetle *Hemipharis insularis*. Here, almost all the polarization reflected from the beetle is left hand circularly polarized and is coded with purple. Notice the radial symmetry of elliptically polarized light on the body of the beetle.

Journal of Experimental Biology • Supplementary information